

CHAPTER 5.

EXPERIMENTAL RESULTS: SHEAR PARTITIONS

5.1. Overview

The distribution of shear stresses, both local and spatially averaged, is of particular interest in open-channel flows as it provides insight into both the nature of the flow and the capacity of the flow to move sediment. With bedforms present, Reynolds stress profiles have been shown from laboratory experiments to be different from those in flat-bed situations (Bennett and Best, 1995; Nezu and Nakagawa, 1993). The nature of the local shear stress distribution is of some importance in understanding the dominant mechanisms of flow separation, boundary-layer development, and potential flow. A conceptualization of the evolution of the local shear-stress behavior in flow over bedforms is given in figure 5.1. Shear-stress distributions observed in the laboratory experiment of Nelson and others (1993) are shown in figure 5.2.

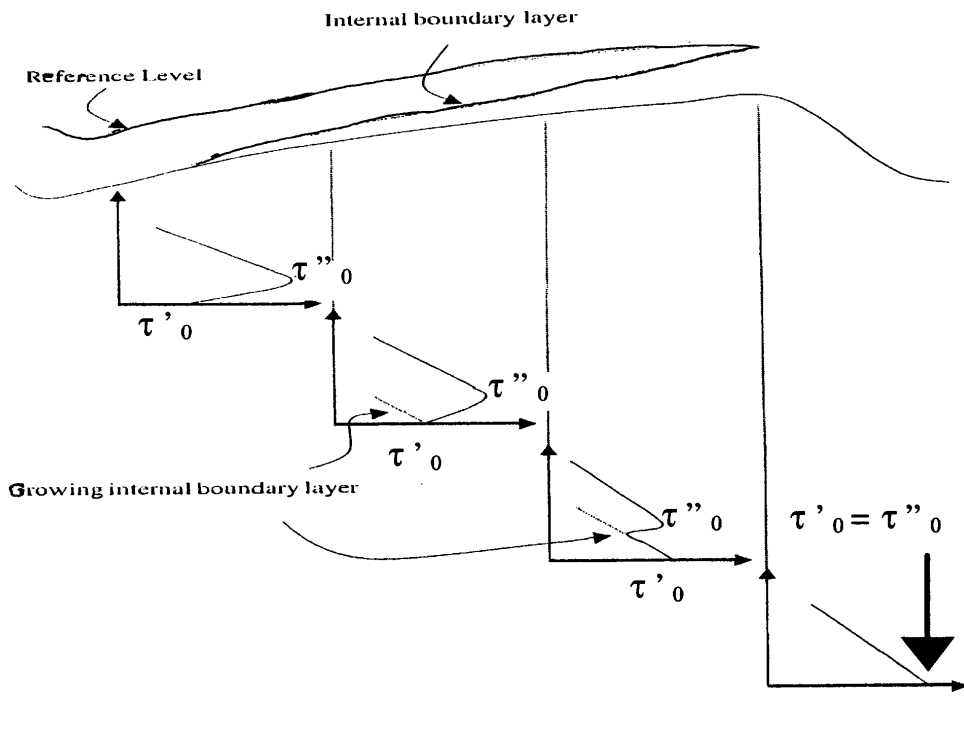


Figure 5.1—Evolution of the shear-stress distribution as proposed by Fedele and Garcia (2001)

A conceptualization of the generalized appearance of the spatially averaged shear-stress profile as proposed by Fedele and Garcia (2001) is illustrated in figure 4.44. Two distinct regions of flow are present (corresponding to different scales of the flow), with the separation point between the layers corresponding to a maximum in the Reynolds stress. Fedele and Garcia (2001) refer to this interface level as the equilibrium level ($z = \varepsilon_e$), whereby at this location they assume that the velocity profiles from the two regions of flow match; there is negligible vertical momentum transfer, and that the velocity at this equilibrium level is equal to the vertically averaged mean velocity. The two regions of flow and the associated velocity and shear-stress distributions are illustrated in figure

4.44. The peak shear stress is assumed to occur at the equilibrium level, with the value of the shear stress at that point equal to the form shear stress (τ_0''). The value of the shear stress in its intersection with the bed is proposed to be equal to the grain shear stress (τ_0').

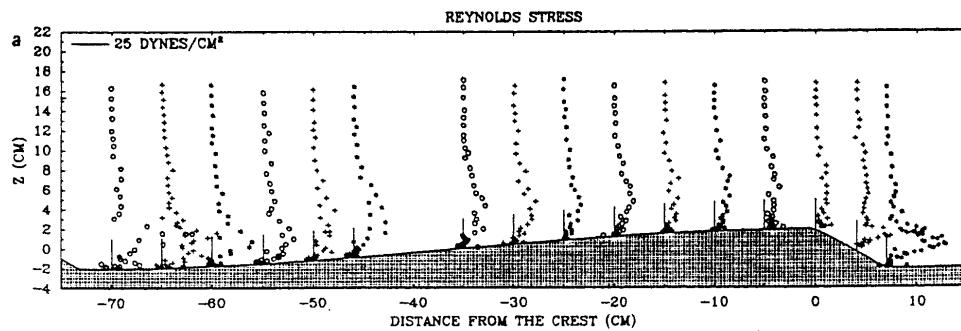


Figure 5.2---Measurements of Reynolds stress over a laboratory dune (Nelson and others,1993)

Because ADCP beam velocities were not digitally stored¹, the KANK-1 and MO-1 data sets have Reynolds stress data only for those locations where ADV data were collected. Thus, it is difficult to make many definitive statements regarding shear-stress distributions for these data sets. For the MO-2 data set, ADV data were collected at numerous points at each vertical, allowing good definition of Reynolds stresses throughout the water column. In addition, as a backup, beam velocities were stored for MO-2 data sets, which allows computation of the Reynolds stress from the ADCP data.

¹ A special command must be given to the RD Instruments Rio Grande ADCP to store beam velocities, as this is not done automatically. Beam velocities are required to compute Reynolds stress in the methods outlined in Stacey and others (1999) (see equation 3.1).

This chapter attempts to provide insight into two main issues: 1) how does the shear-stress profile found in laboratory experiments compare with that found in the field, and 2) how do current shear-partition models compare with field data. To look into these issues, Reynolds stress data is supplemented by estimates of local shear stress at the bed computed from the local shear velocity (which can be computed from the local velocity profile) along with use of the bulk shear stress (τ_0) computed from the product of the water slope and average flow depth. In addition, the value of the coefficient, C_d , found in the form drag closure will be evaluated.

5.2. Shear Stress Field Data

The local shear-stress distributions from ADV data in the MO-2 experiment are presented in figure 5.3, with more detailed “close-ups” of the individual data shown in figures 5.4-5.6. The MO-2 data and the laboratory data of Nelson and others (1993) (figure 5.2) and Bennett and Best (1995) are similar, with the stress increasing away from the bed in the near-bed wake regions behind the superimposed dunes, reaching a maximum near the center of these wake regions and then decreasing to the water surface. The diffusion of the wake shear is evident in the evolution of the shear profile from $X=28$ m to $X=58$ m, although the presence of smaller dunes along this length clouds the picture of shear profile relation with bed profile. In general, the highest shear stresses are in the flow-separation zones and along the shear layer, as also was noted in the laboratory data of Bennett and Best (1995).

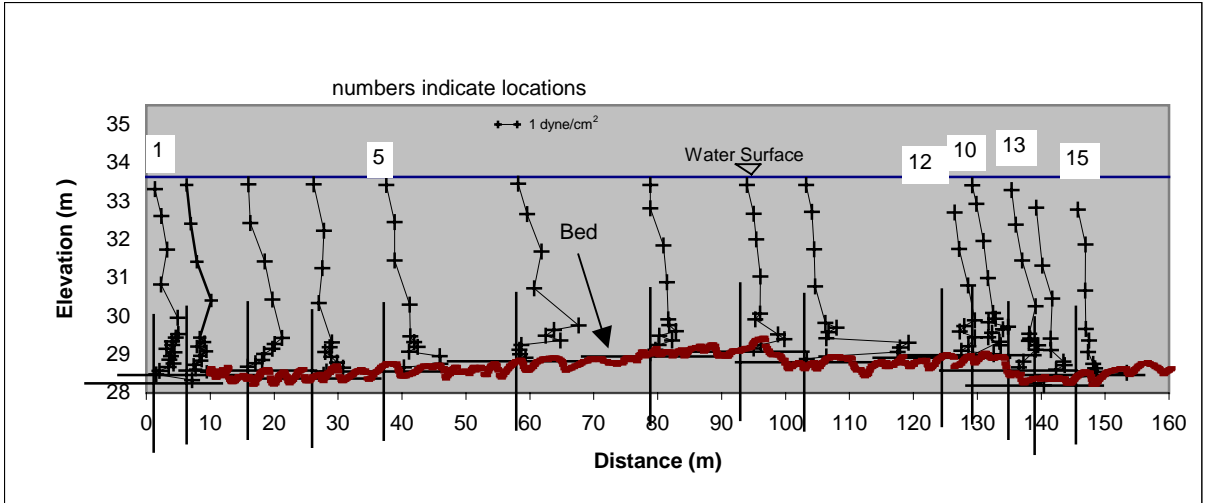


Figure 5.3—Reynolds stress measurements from MO-2, at locations 1-15, with location 11 omitted

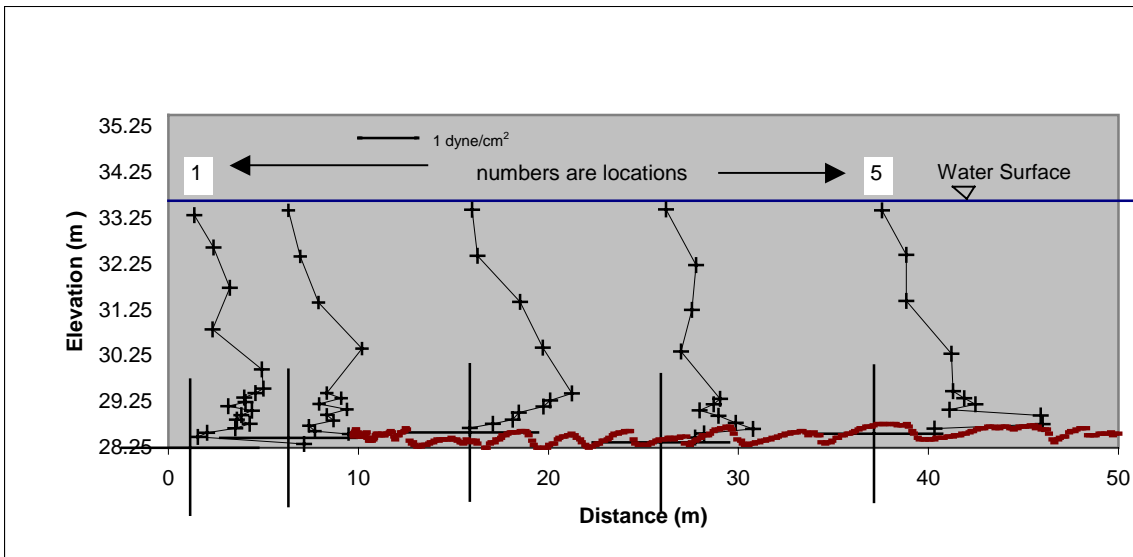


Figure 5.4—Reynolds stress measurements for $0 < x \leq 50$ meters of the MO-2 profile, showing locations 1-5

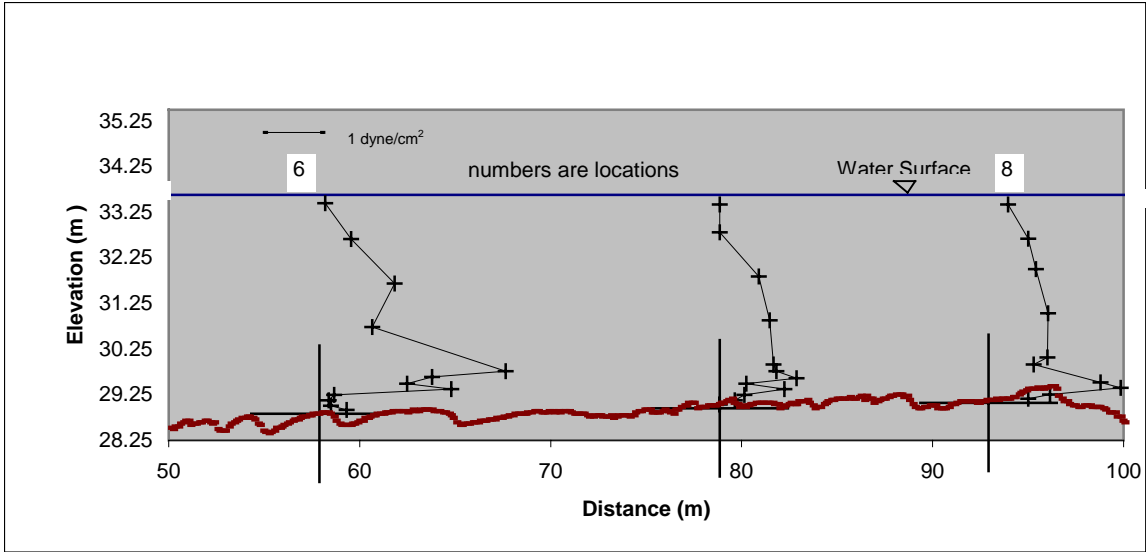


Figure 5.5—Reynolds stress measurements for $50 \leq x \leq 100$ meters of the MO-2 profile, showing locations 6-8

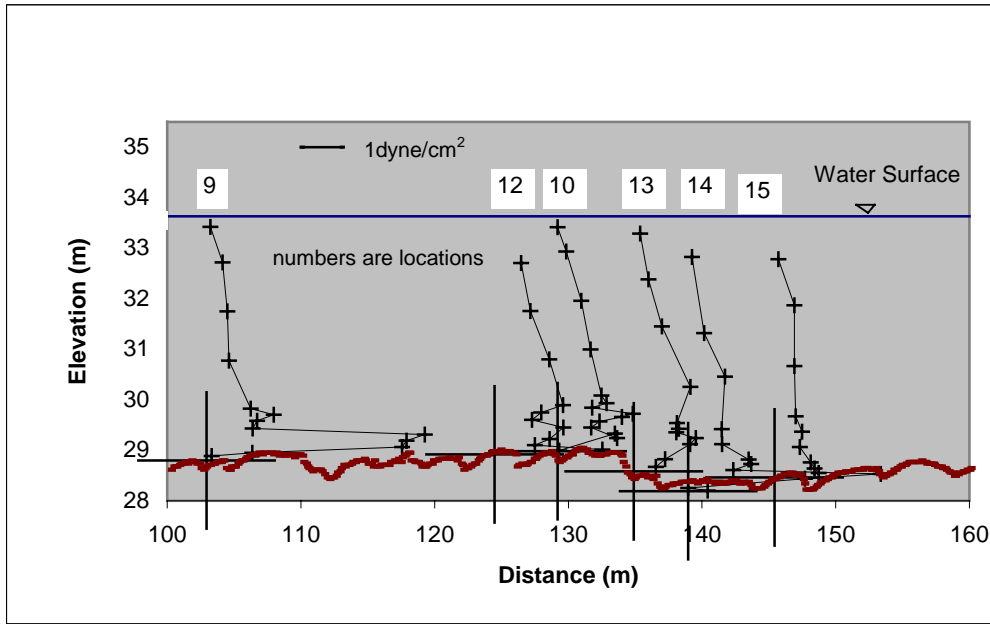


Figure 5.6—Reynolds stress measurements for $100 \leq x \leq 160$ meters of the MO-2 profile, showing locations 9-15, except location 11

Spatial averaging of the Reynolds stresses along lines equidistant from the boundary for experiments KANK-1 and MO-2 are found in figures 5.7 and 5.8, respectively (Reynolds stress data for MO-1 are not available). Although KANK-1 only had 3 ADV points (plus the water surface where $\tau=0$), there is good indication that the shear stress distribution is nearly identical to equilibrium flat-bed flow, with a monotonically decreasing shear stress away from the bed. This similarity with flat-bed flow is consistent with the nature of the bedforms present on the KANK-1 bed (extremely long bedform length and small lee slope). No discernable flow separation was present in the KANK-1 flow and the dune field was elongated, asymmetric, with a low ratio of dune height to flow depth.

The MO-2 data are similar to the laboratory studies for flow over dunes, as the shear stress increases from the bed to a maximum at around 0.5 m elevation, then decreases to the water surface. Comparison of laboratory and the MO-2 spatially averaged Reynolds stress distributions (figure 5.9) indicates good similarity in the bottom half of the flow when shear stress is nondimensionalized by dividing by the product of the density and the mean velocity squared. In the upper half of the flow, the MO-2 data have a nearly linear decrease in shear stress to near zero at the water surface. The laboratory data do not show this same decrease to zero near the water surface, but approach zero well below the water surface in both data sets. As noted by Nelson and others (1993), this result is because of a lack of equilibrium flow conditions, as the flow nearly is inviscid above the point, where the shear stress goes to zero. Equation 2.85 (restated here) is the momentum equation in the x direction can be simplified and given as:

$$u \frac{\partial u}{\partial x} + w \frac{\partial u}{\partial z} = -\frac{1}{\rho} \frac{\partial p}{\partial x} + gS - \frac{\partial \overline{u'w'}}{\partial z} \quad [2.85]$$

where S is the bed slope, p is the pressure, $\overline{u'w'}$, when multiplied by the density, ρ , is the Reynolds Stress or turbulent stress described in equation 2.63. For steady-uniform equilibrium flow, the assumption is that the inertial terms (left-hand-side) and the pressure gradient are negligible as $\frac{\partial}{\partial x} = 0$ and $w = 0$. As pointed out by Nelson and others (1993), for even small deviations from equilibrium, the mean-flow momentum flux in the vertical (second term on the left side) is of the same order of magnitude as the gravitational (gS) and shear-stress divergence $\left(\frac{\partial \overline{u'w'}}{\partial z} \right)$ terms, causing the shear stress to go to zero below the water surface (figure 5.4). However, for the MO-2 data set, the upper flow region approaches a quasi-equilibrium condition, which Nelson and others (1993, p 3944) assumed might result for longer reaches.

The shear-stress partition data from the two Missouri River data sets are given in table 5.1 (the Kankakee River data set was not partitioned as the Reynolds stress data indicates the flow is behaving as a flat-bed flow (figure 5.7)). The total or bulk shear stress is the product of the unit weight of water, the average depth, and the water-surface slope. The grain-shear stress is computed as the average of the near-bed local shear stresses from the near the point of reattachment to the point of separation (taken as the bedform crest). Wiberg and Nelson (1992) were interested in the mechanisms that control sediment transport and make the argument that “*the boundary shear stress, and hence sediment transport, on the stoss side of a bedform are directed downstream only between the*

reattachment point and the crest, it is over this region that boundary shear stress is averaged.” The grain-shear stress is the part of the shear partition that moves the sediment as the form shear stress results from “*a net pressure distribution over an entire bedform*” and is, thus, “*ineffective in moving bedload or entraining sediment*” (Garcia, 1999). An estimate of the local near-bed shear stresses is determined by regression of the velocity profile in the bottom 20% to 25% of the flow depth. A better estimate of the local near-bed shear stress would be to conduct linear regression only on that part of flow depth that is contained within the developing boundary layer (Nelson and Smith, 1989B). A method for determining the top of the developing boundary layer would be to examine the velocity profile and determine in log form where the profile is slightly convex downstream (because of acceleration of the internal boundary layer on the stoss side of the bedform) (Nelson and Smith, 1989B). The data from this field study are not as detailed as data that can be collected in a laboratory environment. It is difficult to determine convexity of the field data at the refinement needed by the Nelson and Smith (1989B) method. In the case of MO-2, with all the superimposed dunes, the velocity profiles used to compute the grain shear stress were those that approximately would simulate the developing boundary layer if only the larger dune were present. Finally, form-shear stress is estimated as the difference between the bulk-shear stress and the grain-shear stress. These estimates, although approximate, will be used to obtain the relative performance of the various shear-partition theories/models.

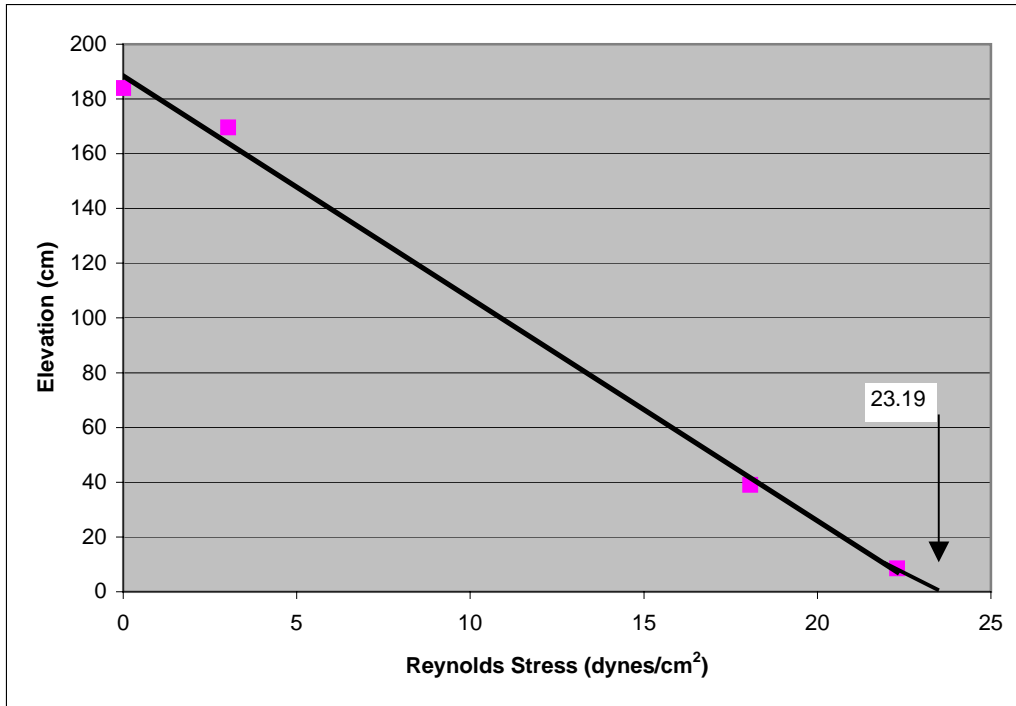


Figure 5.7—Spatial average of the Reynolds stresses for the KANK-1 data by averaging along lines of equal distance from the bed

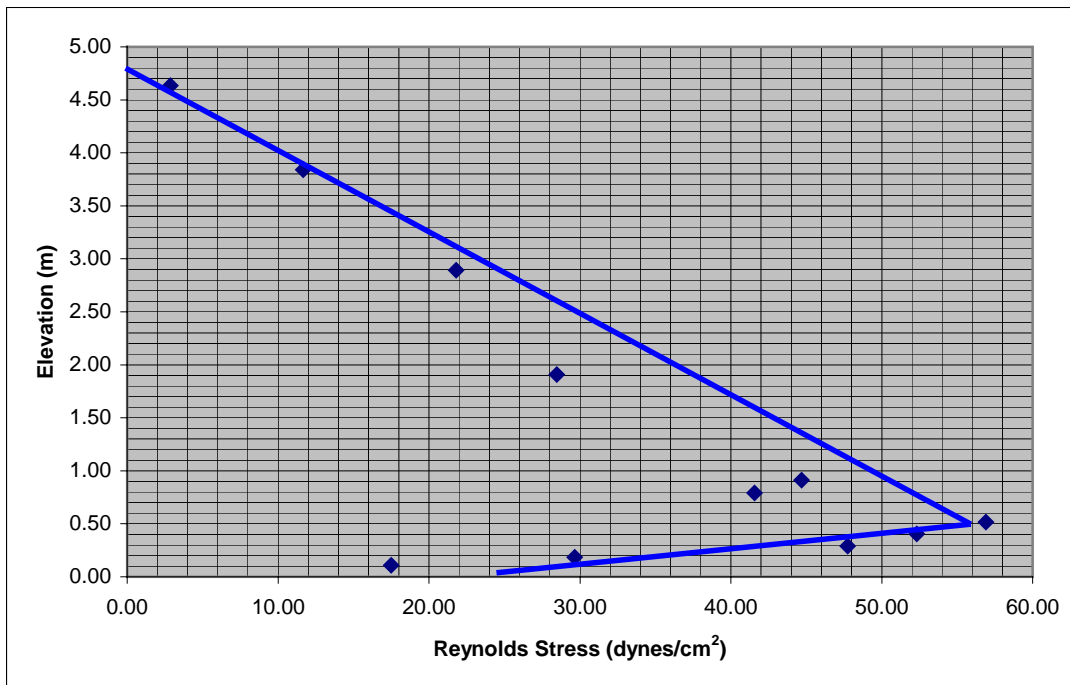


Figure 5.8—Spatial average of the Reynolds stresses for the MO-2 data by averaging along lines of equal distance from the bed

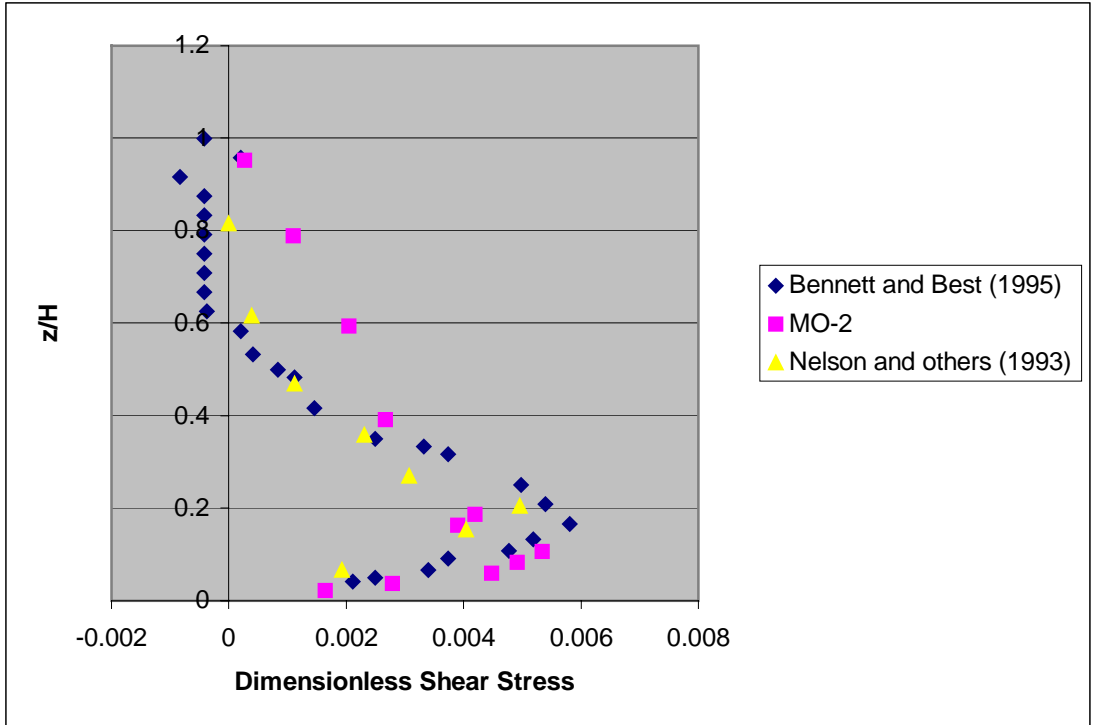


Figure 5.9—Dimensionless spatially averaged shear stress and elevation

DATA SET	τ_0 (dynes/cm²)	τ_0' (dynes/cm²)	τ_0'' (dynes/cm²)
MO-1	99.20	32.38	66.82
MO-2	81.18	24.60	56.58

(τ_0 = total or bulk shear stress, τ_0' =grain shear stress, τ_0'' = form shear stress)

Table 5.1—Shear-stress partition values for the MO-1 and MO-2 data

The conceptualization of the shear partition by Fedele and Garcia (2001) (figure 4.44) can be evaluated in light of the detailed shear-stress distribution data of MO-2 (figure 5.8). Fedele and Garcia propose that the location of the maximum shear stress corresponds to both the equilibrium level and the approximate form shear stress, whereas

the intersection of the shear-stress distribution with the bed roughly corresponds to the grain shear stress. Fedele and Garcia (2001) come up with this postulation based on laboratory observations and the work of Lopez and Garcia (1999), where Lopez and Garcia used wall-similarity assumptions to propose that the extrapolated intercept of the Reynolds stress with the bed was equal to the grain shear stress, irrespective of bed roughness. Fedele and Garcia (2001) discuss how this locus of shear stress maximum “*indicates the relevant processes in turbulence and shear stress production, that is wake propagation and shear-layer diffusion, and purely wall-related turbulence.*”, however, the author can find no physical reasoning behind why Fedele and Garcia (2001) equate the spatially averaged shear stress maxima to the form shear stress, other than laboratory observation. Smith and McLean (1977, p. 1743) note that the increase of the shear stress away from the boundary (in the immediate vicinity of the boundary) is caused by the “*z dependent pressure gradient*” (topographically induced pressure distribution). It is reasonable to believe that by spatially averaging the shear-stresses, that the maximum of the spatial average would equal the form shear stress, which is an integration of the pressure gradient features over the reach.

The flow velocity at the equilibrium level also is assumed to be equal to the mean velocity, which through the reasoning of Fedele and Garcia (2001) would imply that turbulence production becomes negligible above the equilibrium layer, with

$$\int_{\varepsilon}^H \frac{\tau(z)}{\rho} \frac{du}{dz} dz + u_{*T}^2 u_{\varepsilon} = u_{*T}^2 U \quad . \quad [5.1]$$

The blue line shown on figure 5.8 is how the Fedele and Garcia (2001) conceptualization would appear using the form and grain shear stresses computed for MO-2 (table 5.1). The equilibrium level was estimated based on the appearance of a discontinuity in the velocity plots in figure 4.30C. There is a remarkably good fit between the observed data and the conceptualization. However, the measured velocity at the equilibrium layer is 69 cm/s (figure 4.30C), which almost is 40 cm/s less than the mean, flow velocity of 102.93 cm/s (table 4.1). This disparity indicates that the turbulence production above the equilibrium level is not negligible (equation 5.1) and contributes much to the total mean-flow energy loss (as much as 30% of the contribution occurs above the equilibrium level in this data set). This assumption used by Fedele and Garcia (2001) likely is a major contributor to the poor performance of their velocity model (Section 4.7). The validity of the Fedele and Garcia (2001) conceptualization for the spatially averaged shear-stress distribution is not dependent on the associated velocity distribution conceptualization (it was based on laboratory observation). However, any computation of the shear stress partition is jeopardized by the incorrect velocity model assumptions.

Fedele and Garcia (2001) based much of their postulation on the flume data from Bennett and Best (1995). It is possible that the turbulent scale differences are large enough between the large river and the laboratory flume to induce a greater percentage of turbulence production in the outer region for large rivers than for the flume. The MO-2 data have Reynolds stresses approaching zero at the water surface as opposed to the laboratory data, which show a decrease to zero shear stress well below the water surface.

This decrease lends support to the idea that the turbulence production in the outer region for field-scale flows is larger as turbulence production, $\int \frac{\tau(z)}{\rho} \frac{du}{dz} dz$, is dependent on shear stress. However, because of the natural sinuosity of field-scale flows, it must also be acknowledged that other factors, such as secondary currents (Nezu and Nakagawa, 1993, p. 85), may influence the outer-flow region shear-stress distribution.

The spatially averaged shear-stress distribution for MO-2 presented in figure 5.8 was computed by averaging along lines of equal distance from the bed at each location. Bennett and Best (1995) estimated the total shear stress as the spatial average of the local shear stresses along lines of equal elevation above a mean bed elevation for the developing boundary layer. The intersection of the spatially averaged shear-stress distribution and the mean bed elevation was estimated as the total shear stress (figure 5.10). To determine the validity of this estimation method for field data, the shear stress data from the MO-2 data set were averaged in this same manner (figure 5.11). The intersection of the spatially averaged shear-stress distribution and the mean bed elevation differed by more than 35% in comparison to the estimated total bed shear stress (81.18 dynes/cm²) given for the MO-2 experiment in table 5.1.

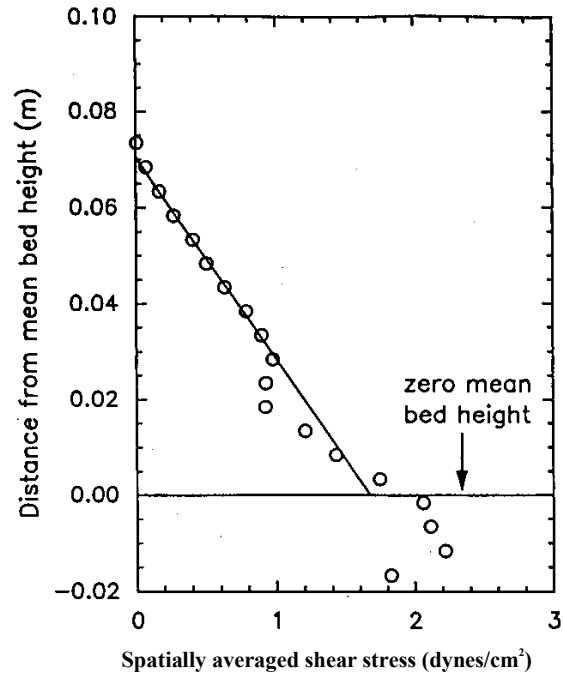


Figure 5.10— Spatial average of the Reynolds stresses for the Bennett and Best flume data by averaging along lines of equal distance above the mean bed elevation (Bennett and Best, 1995)

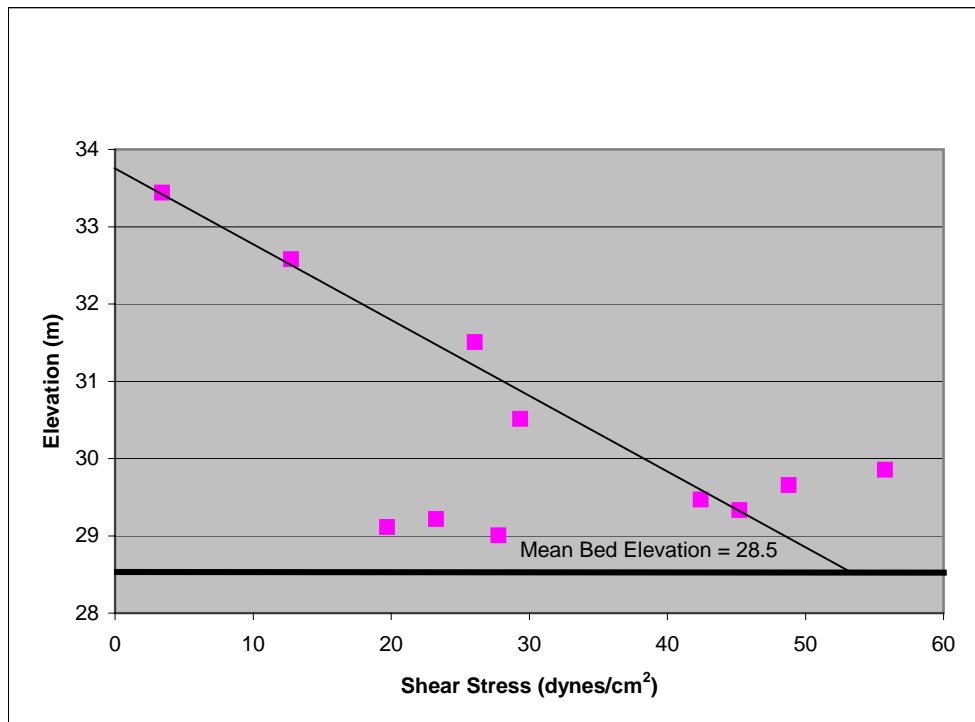


Figure 5.11-- Spatial average of the Reynolds stresses for the MO-2 data by averaging along lines of equal distance above the mean bed elevation

5.3. Evaluation of Available Shear Partition Models with Field Data

In alluvial rivers, shear partitioning is important in the computation of sediment transport, as grain shear stress is the predominant driving force for the resuspension and transport of sediment particles. In addition, for computation of the stage-discharge relation, it is critical to understand the additional resistance imparted by the presence of bedforms.

Two shear partition models (Einstein (1950) and Nelson-Smith (comes collectively from Smith and McLean, 1977; Wiberg and Nelson, 1992; and Nelson and others, 1993)) will be evaluated. The method of Einstein (1950) requires no knowledge of bedform dimensions, unlike the Nelson-Smith method, that requires knowledge of bedform geometry.

The method of Einstein (1950) was the first method to partition the shear stresses. Garcia (1999) elucidates the Einstein method development in a much clearer and understandable manner than the original discussion contained in Einstein's original paper. Thus, much of Garcia's (1999) discussion is utilized to explain the method here. The frictional resistance coefficient in equation 1.4, under Einstein's theory, represents the resistance because of both grain and form effects. Einstein postulated that the grain resistance could be computed as

$$\tau_0' = \rho C_{fs} U^2 \quad , \quad [5.2]$$

where C_{fs} is the frictional resistance attributable to the grains. Recalling that Keulegan's relation for rough flow is

$$\frac{U}{u_*} = \frac{1}{\kappa} \ln\left(\frac{11H}{k_s}\right) , \quad [5.3]$$

where U is the mean velocity, an assumption is made that this equation can be altered to become

$$\frac{U}{u'_*} = \frac{1}{\kappa} \ln\left(\frac{11H'}{k_s}\right) , \quad [5.4]$$

where u'_* is the grain shear velocity and H' is the flow depth that would occur in the absence of bedforms. If uniform flow is assumed, from equation 2.55 and following Einstein's previously established line of reasoning, the grain shear stress is expressed as

$$\tau'_0 = \rho g H' S . \quad [5.5]$$

Utilizing equations 1.7, 5.4, and 5.5, the portion of the depth attributable to the grain-shear stress is

$$H' = \frac{U^2}{gS} \left[\frac{1}{\kappa} \ln \left(\frac{11H'}{k_s} \right) \right]^{-2} . \quad [5.6]$$

Assuming that the flow geometry, sediment bed-material characteristics, and mean velocity are known, Einstein's method proceeds in the following steps.

1. Assume some relation to compute k_s , such as $k_s = 2.5 D_{50}$.
2. Iteratively compute H' from equation 5.6.
3. Compute the grain shear stress from equation 5.5.
4. The total shear stress can be computed from equation 2.55 as the water slope and average flow depth are known.
5. Compute the form shear stress from equation 2.41.

The method of Nelson-Smith has been explained previously in Section 2.2. Equations 2.52, 2.53, and 2.54 are of primary importance and are restated below for convenience.

The form shear stress can be computed from the form drag divided by the area of the bed over which the force is applied as

$$\tau_0'' = \frac{1}{2} \rho C_d \frac{H_d}{\lambda} U_r^2 , \quad [2.52]$$

where C_d = drag coefficient (assuming 0.25 from the work of Smith and McLean, 1977),

H_d is the dune height, U_r denotes the reference velocity (corresponding to the mean

velocity between $z = k_s$ and $z = H_d$ if the dunes were not present), and λ is the bedform wavelength. From integration of the logarithmic velocity profile, U_r is given by the following equation as

$$\frac{U_r}{u_*'} = \frac{1}{\kappa} \left[\ln \left(30 \frac{H_d}{k_s} - 1 \right) \right] . \quad [2.53]$$

Combining these two equations and assuming partitioning of the shear stress according to that of Einstein (1950) yields

$$\tau_0'' = \tau_0 - \tau_0' = \frac{1}{2} C_d \frac{H_d}{\lambda \kappa^2} \left[\ln \left(30 \frac{H_d}{k_s} - 1 \right) \right]^2 \tau_0' . \quad [2.54]$$

Equation 2.54 can be reduced further to

$$\frac{\tau_0}{\tau_0'} - 1 = \frac{1}{2} C_d \frac{H_d}{\lambda \kappa^2} \left[\ln \left(30 \frac{H_d}{k_s} - 1 \right) \right]^2 . \quad [5.7]$$

Assuming that the flow geometry, dune geometry, and sediment bed material characteristics are known, the Nelson-Smith method proceeds in the following steps.

1. Assume some relation to compute k_s , such as $k_s=2.5 D_{50}$.
2. Compute the total shear stress from equation 2.55.
3. Compute the grain shear stress from equation 5.7.
4. Compute the form shear stress from equation 2.41.

The results from applying the two shear-partition models to the two Missouri River field data sets collected as part of this research are given in tables 5.2 and 5.3. Einstein's method had an absolute average percent error of 11.3%, whereas the Nelson-Smith method had an absolute average percent error of 22.2% when the smaller bedforms were used as the geometry in the Nelson-Smith method. The Einstein method performed particularly well with the MO-1 data set with a +1.0% error in estimating the form shear stress. Obviously, these error percentages are relative to shear partition numbers that are produced through the assumption that the grain shear stress can be estimated effectively by averaging the shear velocities estimated from the local velocity profiles measured in the developing boundary layer. The rationale for this method is discussed in Section 5.2.

Through examination of the Nelson-Smith results for MO-2, it is clear that the better model fit comes when the smaller superimposed dunes are used as bedform geometry input parameters. This better fit possibly implies that the smaller superimposed dunes are the controlling feature in regards to the generation of form shear stress.

DATA SET	Obs.	E	%	N-S		% Error	
	τ'_0 (dynes/cm ²)	τ'_0 (dynes/cm ²)	Error	τ'_0 (dynes/cm ²)			
MO-1	32.38	34.57	+6.8	20.14			-37.8
MO-2	24.60	18.21	-26.0	<u>Large</u> 51.64	<u>Small</u> 19.74	<u>Large</u> +110	<u>Small</u> -19.8

(Obs, observed value; τ'_0 is the grain shear stress; E, Einstein Method; N-S, Nelson-Smith Method; The N-S method used a $C_d = 0.25$)

Table 5.2—Grain-shear stress computed by the shear-partition methods of Einstein (1950) and Nelson-Smith (collectively from Smith and McLean, 1977; Wiberg and Nelson, 1992; and Nelson and others, 1993)

DATA	Obs.	E	%	N-S		% Error	
	τ''_0 (dynes/cm ²)	τ''_0 (dynes/cm ²)	Error	τ''_0 (dynes/cm ²)			
MO-1	66.82	67.46	+1.0	81.89			+22.6
MO-2	56.58	63.01	+11.4	<u>Large</u> 29.57	<u>Small</u> 61.47	<u>Large</u> -47.7	<u>Small</u> +8.6

(Obs, observed value; τ''_0 is the form shear stress; E, Einstein Method; N-S, Nelson-Smith Method; the N-S method used a $C_d = 0.25$)

Table 5.3—Form-shear stress computed by the shear-partition methods of Einstein (1950) and Nelson-Smith (collectively from Smith and McLean, 1977; Wiberg and Nelson, 1992; and Nelson and others, 1993)

When evaluating the sensitivity of the drag-coefficient parameter, C_d , in the Smith-Mclean model, a lesser effect is found than would first be assumed. For example, doubling the drag coefficient (from 0.25 to 0.50) only resulted in a 10% change in the final value of form stress for the MO-1 data. Nonetheless, it is worthwhile to use the

present field data from this research to evaluate the value of the drag coefficient.

Equation 5.7 can be manipulated to allow computation of the drag coefficient. C_d is shown in table 5.4 for the two Missouri River experiments, MO-1 and MO-2 (note: KANK-1 was not included, as the flow approximated a flat-bed flow)

Data Set	$(z_0)_n$	C_d
MO-1	0.0025 cm	0.14
MO-2	0.0025 cm	0.21

Table 5.4—Estimated drag coefficients

The drag coefficients for MO-1 and MO-2 are close to the values found in the literature, which range from 0.21 (Smith and McLean, 1977) to 0.23 (Wiberg and Nelson, 1992) to 0.25 (Nelson and others, 1993). Both MO-1 and MO-2 flows separated. Smith and McLean (1977) conclude that for scenarios with no flow separation, a higher drag coefficient is warranted and suggested $C_d=0.84$. This conclusion seems counterintuitive to the author, as the higher drag coefficients would stem from additional flow separation (drag coefficient is proportional to the drag force; equation 2.51). Nelson and others (1993, p. 3,944) suggest that the interaction of spatial acceleration of the flow over dunes with the turbulence field is important in altering the form drag of bedforms. Nelson and others (1993) saw a marked increase in the drag coefficient in one data set ($C_d=0.45$) with no spatial acceleration effects.

After reviewing the two methods, the author would recommend the Einstein (1950) method over that of Nelson-Smith. This recommendation is based on both the better relative error estimates for Einstein and the need for bedform geometry in the Nelson-Smith method. As has been demonstrated in Sections 4.2 and 4.3, the bedforms encountered in the field are more complicated than what typically is defined as equilibrium dunes and, thus, prediction of the bedform geometry is difficult for field situations.

5.4 Conclusions

There are similarities in the local shear-stress distribution seen in the field and the laboratory data with the stress increasing away from the bed in the near-bed wake regions behind the superimposed dunes, reaching a maximum near the center of these wake regions and then decreasing to near zero at the water surface. Comparison of laboratory and the MO-2 spatially averaged Reynolds stress distributions indicates good similarity in the bottom half of the flow when dimensionless elevation and shear stress (nondimensionalized by dividing by the product of the density and the mean velocity squared and the density) are used. In the upper half of the flow, the MO-2 data revealed a quasi-equilibrium shear-stress distribution, with the shear stress linearly decreasing to zero near the water surface. The MO-2 shear-stress distribution is unlike the laboratory data, which had shear stress distributions that linearly decreased away from the bed, but became zero well below the water surface, indicating a lack of dynamic equilibrium between the inertial and pressure forces.

The conceptualized spatially averaged shear-stress distribution of Fedele and Garcia (2001) fits the measured MO-2 data well, although the point velocity at the equilibrium level does not correspond to the mean velocity. This result indicates that the turbulence production above this level is not negligible as postulated by Fedele and Garcia (2001). As the Fedele and Garcia (2001) conceptualization is based on laboratory data, it is possible that turbulence generation is much greater in the outer region of river-scale flows than for laboratory-scale flows.

Two methods of shear partitioning: 1) Einstein (1950) and 2) Nelson-Smith (Smith and McLean, 1977; Wiberg and Nelson, 1992; and Nelson and others, 1993) were evaluated against form and grain shear stresses for the Missouri River data sets (MO-1 and MO-2) estimated using a methodology used by Nelson and others (1993). Both of these methods require knowledge of the total shear stress. Einstein's method requires knowledge of the mean velocity, whereas the Nelson-Smith method requires knowledge of the bedform geometry. Einstein's method had an absolute average percent error of 11.3%, whereas the Nelson-Smith method had an absolute average percent error of 22.2% when the smaller bedforms were used as the geometry in the Nelson-Smith method. Through application of the Nelson-Smith model, it is apparent the smaller superimposed dunes are the controlling feature in regards to flow and stress distributions over bedforms. The Einstein (1950) method is recommended over that of the Nelson-Smith method based on both the better relative error estimates being better for Einstein, and the need for bedform geometry in the Nelson-Smith method.

Drag coefficients were computed for each of the Missouri River data sets (MO-1 and MO-2). The drag coefficients for MO-1 and MO-2 data were 0.14 and 0.21, respectively, which are comparable to those determined in other studies (Smith and McLean, 1977; Nelson and others, 1993).